Arch. Metall. Mater. **71** (2026), 1, 187-194

DOI: https://doi.org/10.24425/amm.2026.157780

KUIFANG ZHANG[1,2*], BOHAN WEI[1,2], XIN WEN[1,2], RUIXIANG WANG[2*]

LEACHING KINETICS AND BEHAVIOR OF RARE EARTHS FROM DEEP-SEA MUD WITH SULFURIC ACID

Deep-sea mud is expected to be a novel and potential rare earths resource that supplements terrestrial rare earths, and has received international attention. In this work, the leaching kinetics and behavior of rare earths from deep-sea mud with sulfuric acid was investigated. The results revealed that the rare earth elements (REEs) could be leached out via a sulfuric acid leaching process. A optimized REEs leaching percentage of 82.83% was obtained by using 1.0 mol/L sulfuric acid as leaching agents with a liquid-solid ratio of 4:1 and stirring speed of 250 rpm at 60°C for 30 min. Under the optimized leaching conditions, the leaching kinetics analysis showed that the leaching process was conformed to the shrinking-core model which contained two stages as follows: 1) From 0 min to 4 min, the reaction was controlled through an external diffusion process, and could be described as $X = 0.5491 \cdot e^{-4569/RT} \cdot t$ ($Ea = 4.569$ kJ/mol); 2) From 4 min to 30 min, due to the increase of solid calcium sulfate products, the reaction gradually transformed into an internal diffusion-controlled process, and could be described as $1 - 2/3X - (1 - X)^{2/3} = 0.0577 \cdot e^{-7083/RT} \cdot t$ ($Ea = 7.083$ kJ/mol).

Keywords: Rare earths; Deep-sea mud; Sulfuric acid; Leaching; Kinetics

1. Introduction

Rare earth elements (REEs) are crucial for advanced defense technologies and artificial intelligence systems due to their exceptional magnetic, optical, and electrical properties [1-3] However, decades of extensive extraction and use have significantly depleted terrestrial reserves. To mitigate potential supply chain disruptions and ensure sustainable global market development [4-5], marine REE resources in deep-sea mud have become a central focus of international research, with their total reserves potentially surpassing those of terrestrial REE resources [6-9].

Marine REE resources was formally recognized as the fourth major category of seafloor resources by the 17th session of the International Seabed Authority, alongside polymetallic nodules, cobalt-rich ferromanganese crusts, and seafloor massive sulfides. Marine REE resources primarily refer to deep-sea mud, defined as unconsolidated materials found on the ocean floor at depths exceeding 2,000 meters [10]. The main sources of REE are believed to include marine biological remains, terrigenous material transport, marine volcanic eruptions, and marine autogenetic minerals [11-13]. In 2011, Kato et al. [14] first identified the deep-sea mud of the Pacific Ocean as a promising alternative REE source, documenting high-grade occurrences across the eastern South and central North Pacific basins. Remarkably, a single 1 km^2 area near sampling sites could satisfy 20% of the current global annual demand. Subsequent investigations near Minamitori Island in the western North Pacific confirmed extraordinary REE enrichment averaging 7,000 mg/kg – substantially exceeding terrestrial ore grades and other marine REE sources [15-17]. Comprehensive resource evaluations by Takaya et al. [18] in 2018 demonstrated that a 105 km^2 area with a 10-meter mining depth contains approximately 1.2 million tons of REEs, capable of supplying global annual requirements for Yttrium (62 years), Europium (47 years), Terbium (32 years), and Dysprosium (56 years). Extrapolating to 2,500 km^2, the resource base could exceed 16 million tons – sufficient to meet global demand for centuries. Recent discoveries confirm widespread high-grade REEs mud across the Pacific, Indian, and Atlantic Oceans [19-23], with prime prospects including the Clarion-Clipperton Zone, western Pacific basins, southeast Pacific regions, and the central Indian Ocean-Wharton Basin [24-27].

Despite this promise, current research is predominantly focused on geological surveys and sampling, with limited reports

[1] GANNAN UNIVERSITY OF SCIENCE AND TECHNOLOGY, SCHOOL OF INTELLIGENT MANUFACTURING AND MATERIALS ENGINEERING, GANZHOU KEY LABORATORY OF GREEN EXTRACTION AND HIGH QUALITY UTILIZATION OF REGIONAL CHARACTERISTIC METAL RESOURCES, GANZHOU 341000, CHINA
[2] JIANGXI UNIVERSITY OF SCIENCE AND TECHNOLOGY, COLLEGE OF METALLURGICAL ENGINEERING, GANZHOU 341000, CHINA

* Corresponding authors: zhang_kui_fang@163.com ; wrx9022@163.com

on its hydrometallurgical recovery process. In this work, we systematically investigated the leaching process of REEs from deep-sea mud, employing the most commonly used acid agent, sulfuric acid. This study will contribute to the literature on the utilization of this novel REEs resource.

2. Experimental

2.1. Materials

The deep-sea mud samples, collected from the central Pacific Ocean at a water depth of 5486 meters, were obtained from the Marine Geological Survey Institute in Guangdong province. The samples were air-dried, crushed, and screened to a particle size range of 0.075 mm to 0.15 mm for our study. The main chemical composition of the deep-sea mud was as follows (% w/w): REEs, 0.11; Al, 6.74; Fe, 3.56; Mg, 2.57; Ca, 3.20; Mn, 1.56. The minerals in deep-sea mud mainly contained illte (47.32%, w/w), phillipsite (38.1%, w/w), hydroxyapatite (7.59%, w/w), Mn oxides (3.09%, w/w), and other minerals (3.9%, w/w). Sulfuric acid (analytical grade) was obtained from the Nanjing Chemical Reagent Company.

2.2. Methods

2.2.1. Leaching procedure and calculation

The deep-sea mud have been characterized systematically in our previous research [28], proving that REEs in the deep-sea mud mostly existed in hydroxyapatite mineral by partly replacing Ca, thus, the REEs loaded hydroxyapatite minerals can be expressed as $[(Ca)_{10}(REE)(PO_4)_7(OH)_2]$, the leaching reaction was shown as Eq. (1).

$$(Ca)_{10}(REE)(PO_4)_7(OH)_2 + 2H^+ + 10SO_4^{2-} \rightarrow 10CaSO_4 \downarrow + 7PO_4^{3-} + 2H_2O + REE^{3+} \quad (1)$$

The leaching process was carried out in a beaker (Beijing BOMEX Glass Company), which was placed in a temperature-regulated water bath. The water bath was equipped with a magnetic stirrer and a temperature sensor (Changzhou Aohua Instrument Company). Dried deep-sea mud samples and sulfuric acid solution were added in sequence according to the specified dosages. The leaching reactions were driven by magnetic stirring at a constant speed. After the tests, the slurry was vacuum filtered, the obtained residue was promptly rinsed with deionized water and dried under vacuum. The metal content in the residue was quantitatively analyzed to determine the leaching percentage, using Eq. (2). Systematic investigations were performed to evaluate the effects of acid concentration, liquid to solid ratio, reaction time, and reaction temperature, aiming to establish the optimal operational conditions.

Leaching rate (X) was calculated as

$$X = \left(\frac{C_{[M]}V}{\omega_{[M]}S} \right) \quad (2)$$

Here $C_{[M]}$ is the M content in the pregnant leach solutions (g/L); ω[M] is the initial Me mass fraction in the mud prior to leaching (%/100); S is the weight of the mud before leaching (g); and V is the volume of the leach solutions (L); M can be replaced with Al, Fe, Mg, Ca, Mn, or REEs in these equations.

2.2.2. Leaching kinetics

The sulfuric acid leaching process of deep-sea mud is a typical liquid-solid reaction. The volume of the reacted minerals gradually decreased and the solid phases with products formed as the leaching process proceeds. Thus, when the ore particle is regarded as spherical type, the reaction process can be described using the shrinking-core model [29]. During the practical leaching process, the overall reaction rate is determined by the slowest controlling step, and it could be classified as chemical reaction control, internal diffusion control and external diffusion control. When the leaching process is under chemical reaction control, internal diffusion control, or external diffusion control, the kinetic equation can be expressed as Eq. (3), Eq. (4), and Eq. (5), respectively [29-31].

$$1 - (1 - X)^{\frac{1}{3}} = k_1 t \quad (3)$$

$$1 - \frac{2}{3}X - (1 - X)^{\frac{2}{3}} = k_2 t \quad (4)$$

$$X = k_3 t \quad (5)$$

where k_1, k_2, and k_3 are the reaction rate constants, min^{-1}; t is the leaching time, min. X is the leaching rate of REEs corresponding to the leaching time t.

Furthermore, to calculate the activation energy, a plot of ln k vs $1/T$ should be a straight line with a slope of $-Ea/R$ and an intercept of ln$k$ with Arrhenius equation as Eq. (6):

$$\ln k = \ln A - Ea/(RT) \quad (6)$$

where k is the reaction rate constant, min^{-1}; A is the preexponential factor, min^{-1}; R is the mole gas constant, 8.314 $J.mol^{-1}K^{-1}$; T is the thermodynamic temperature, K; Ea is the apparent activation energy, J/mol.

3. Results and discussion

3.1. Batch tests of sulfuric acid leaching

The effects of the sulfuric acid leaching conditions were investigated using a series of batch tests. The results are shown in Fig. 1. Specifically, Fig. 1(a) showed that when sulfuric acid

was used as the leaching agent, the leaching percentage of REEs increased and then decreased with the increase of acid concentration in the range of 0.25-2.0 mol/L, the sulfuric acid concentration corresponding to the peak of the maximum leaching was 1 mol/L. Fig. 1(b) showed that improving the liquid-solid ratio enhanced the leaching. The leaching percentage of REEs increased with the liquid-solid ratio (mL/g) increased from 2:1 to 4:1, and tended to stabilize at the liquid-solid ratio of 4:1. Fig. 1(c) demonstrated that reaction temperature showed a slightly positive effect on leaching, and the leaching percentage of REEs rose smoothly with an increase in temperature. Thus, a temperature of above 60℃ is suitable for the leaching process. Fig. 1(d) showed that the leaching percentage of REEs was significantly affected by the stirring speed. As the stirring speed increased from 50 rpm to 250 rpm, the leaching percentage rose from 56.49% to 83.81%, and then tended to equilibrium. Thus, to ensure the REEs leaching percentage, the stirring speed should be controlled at above 250 rpm. Fig. 1(e) showed that the leaching percentage of REEs increased with the reaction time prolonged to 30 min, and then reached equilibrium, suggesting that controlling the reaction time of 30 min can ensure the sufficient reaction. During the batch tests, non-REEs elements were co-leached out to varying degrees, the overall leaching percentages remained at a relatively low level less than 20%, except for

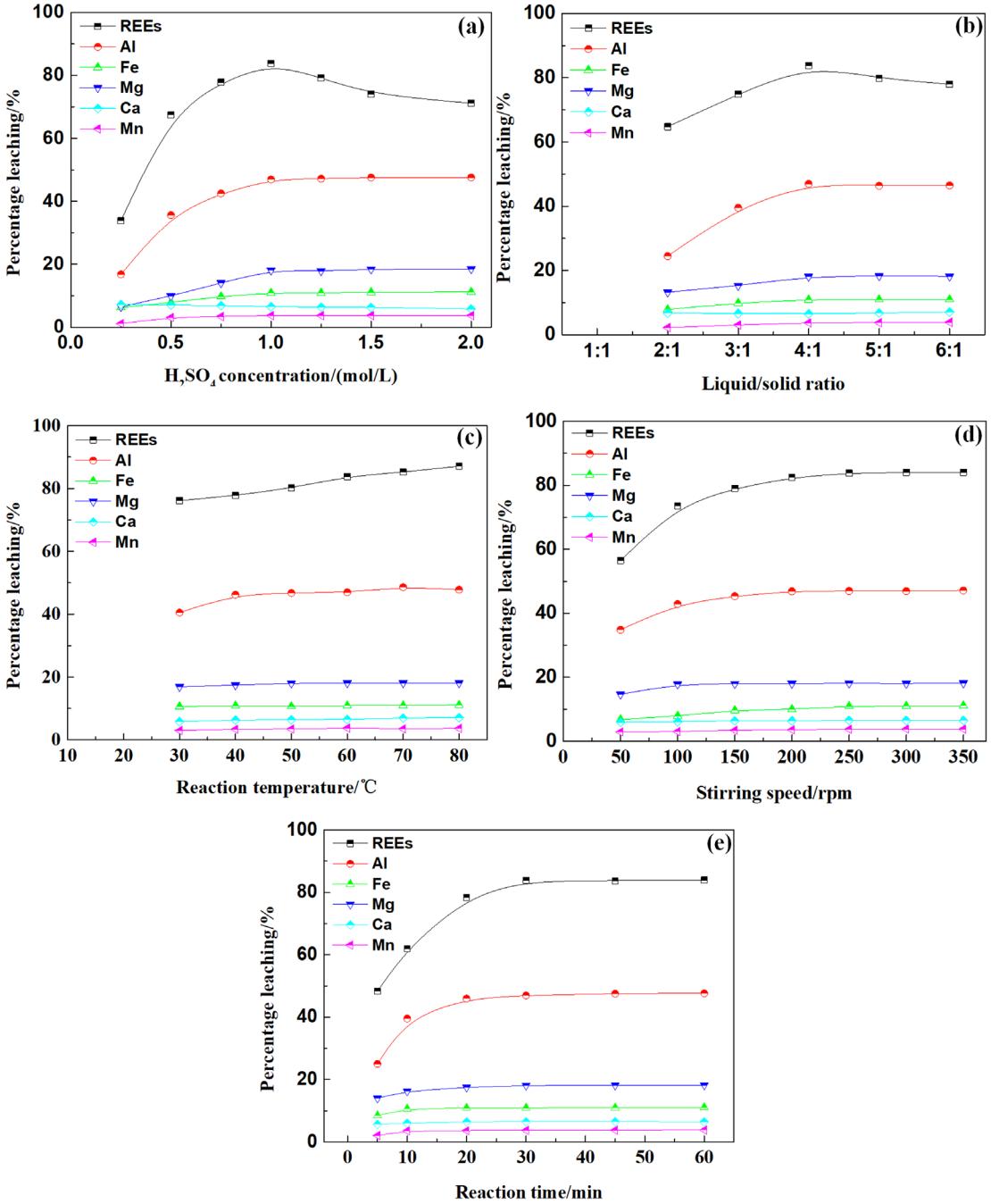

Fig. 1. Effects of different parameters on leaching REEs by sulfuric acid: (a) H_2SO_4 concentration, (b) liquid-solid ratio, (c) temperature, (d) reaction time. Other conditions: leaching agent 1.0 mol/L H_2SO_4, except in (a); liquid-solid volume/mass ratio 4:1 (mL/g), except in (b); reaction temperature 60℃, except in (c); stirring speed 300 rpm, except in (d); reaction time 60 min, except in (e)

Al (nearly 50%). Accordingly, the optimized leaching conditions were determined by using 1.0 mol/L sulfuric acid as the leaching agent with a liquid-solid ratio of 4:1 (mL/g) and stirring speed of 250 rpm at 60℃ for 30 min, resulting in 82.83% of REEs in the deep-sea mud transferring into the leach solutions.

3.2. Leaching kinetics

The leaching kinetics of REEs was investigated at the optimized conditions using a H_2SO_4 concentration of 1.0 mol/L with liquid solid ratio of 4:1 and stirring speed of 250 rpm. The leaching process was conducted with varying reaction times (1, 2, 3, 4, 5, 10, 15, 20, 25, and 30 minutes) at temperatures of 30°C (303 K), 40°C (313 K), 60°C (333 K), and 80°C (353 K) to investigate the relationship between REEs leaching percentages and reaction times under different reaction temperatures, as illustrated in Fig. 2.

As depicted in Fig. 2, the leaching of REEs exhibited a distinct two-stage kinetic pattern. At the first stage of (0-4 min), a pronounced linear increased in the leaching percentage of REEs, suggesting a externally diffusion-controlled. Afterwards, at the second stage of (4-30 min), the leaching rate progression was significantly decelerated and ultimately plateaued. This bimodal behavior implied that the leaching process may be governed by different control mechanisms. Correspondingly, we divided the leaching process into two stages of (0-4 min) and (4-30 min) to conduct the kinetic study, respectively.

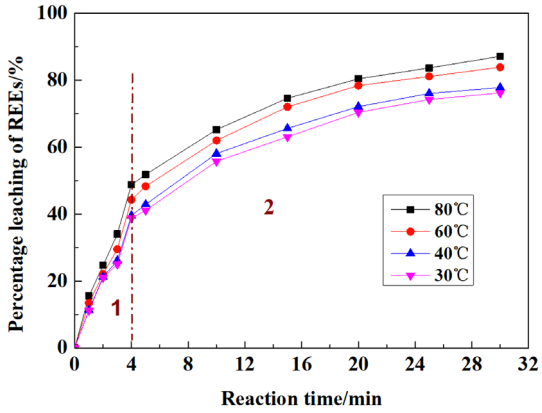

Fig. 2. The relationship between REEs leaching percentages and reaction times under different reaction temperatures.Other conditions: liquid-solid volume/mass ratio 4:1 (mL/g), leaching agent 1.0 mol/L H_2SO_4, and stirring speed of 250 rpm

3.2.1. Leaching kinetics of the first stage (0-4 min)

The leaching kinetics of REEs (0-4 min) was investigated using the shrinking-core model, and the fitting results were shown in Fig. 3. As shown in Fig. 3, The plot of X vs t presented

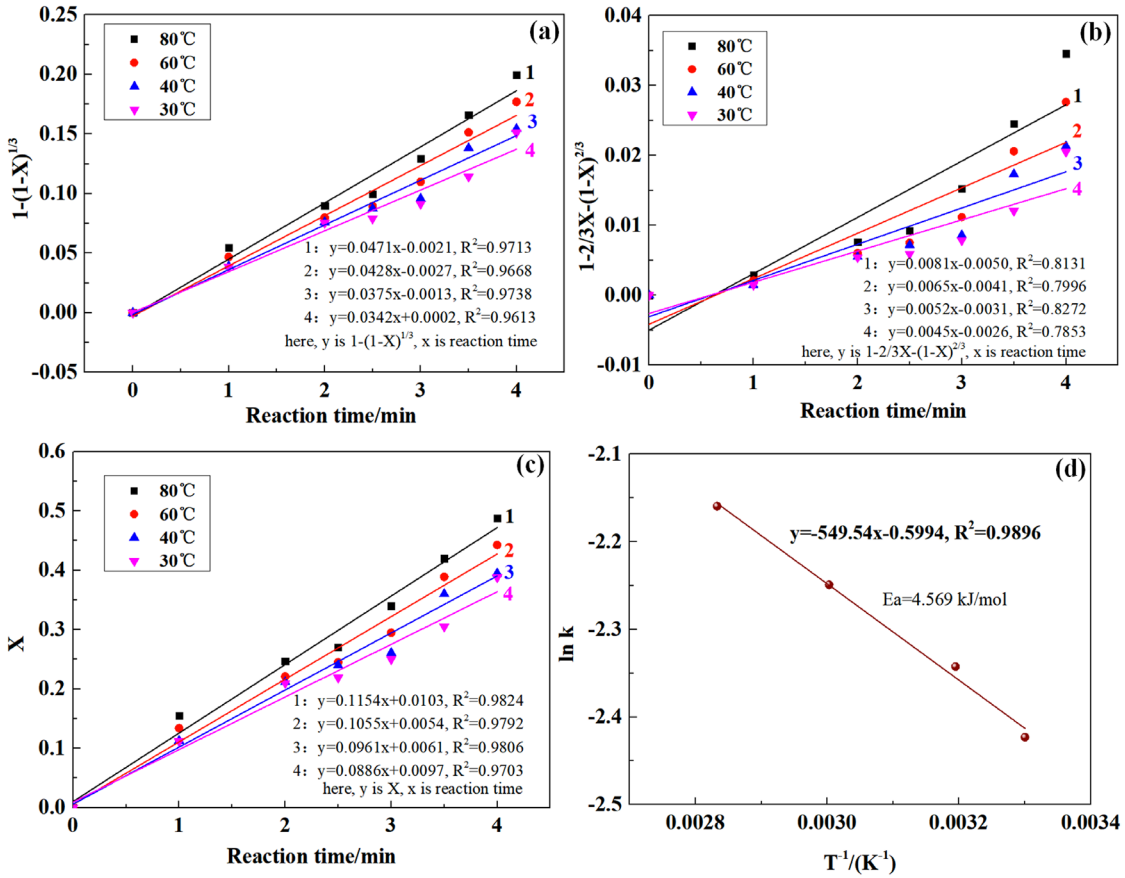

Fig. 3. The results of leaching kinetics for REEs during the sulfuric leaching (0-4 min): (a) Fitting result of $1-(1-X)^{1/3}$ vs t; (b) Fitting result of $1-2/3X-(1-X)^{2/3}$ vs t; (c) Fitting result of X vs t; (d) Calculating activation energy based on Arrhenius Equation

better fitting degree than those of $1-(1-X)^{1/3}$ vs t and $1-2/3X-(1-X)^{2/3}$ vs t, indicating that the process was controlled through external diffusion. According to the fitting result and Arrhenius Equation, activation energy for REEs leaching was calculated as 4.569 kJ/mol. The final leaching kinetics equation for the first stage (0-4 min) can be expressed as: $X = 0.5491 \cdot e^{-4569/RT} \cdot t$.

3.2.2. Leaching kinetics of the second stage (4-30 min)

The leaching kinetics of REEs (4-30 min) was investigated using the shrinking-core model, and the fitting results were shown in Fig. 4. As shown in Fig. 4, The plot of $1-2/3X-(1-X)^{2/3}$ vs t presented better fitting degree than those of $1-(1-X)^{1/3}$ vs t and X vs t, indicating that the process was controlled through internal (product-layer) diffusion. According to the fitting result and Arrhenius Equation, activation energy for REEs leaching was calculated as 7.083 kJ/mol. The final leaching kinetics equation for the first stage (4-30 min) can be expressed as: $1-2/3X-(1-X)^{2/3} = 0.0577 \cdot e^{-7083/RT} \cdot t$.

3.3. Leaching behavior and mechanism

Based on the results of leaching kinetics, the shrinking-core model of hydroxyapatite minerals $[(Ca)_{10}(REE)(PO_4)_7(OH)_2]$ in the deep-sea mud during the H_2SO_4 leaching process was depicted to further clarify the leaching behavior and mechanism. As shown in Fig. 5, the model contained non-leached particle of REEs minerals, internal diffusion layer, external diffusion layer, and leach solutions layer. The main steps of the REEs leaching process can be described as follows: 1) The leaching agent sulfuric acid diffused inward to the surface of the solid film layer of the calcium sulfate product; 2) The leaching agent diffused to the surface of hydroxyapatite minerals through solid film layer of calcium sulfate products; 3) The leaching agent undergoes a chemical reaction with hydroxyapatite; 4) The products of RE^{3+} and PO_4^{3-} diffused from the reaction interface through the solid film layer of calcium sulfate products to the boundary of liquid film layer; 5) The products RE^{3+} and PO_4^{3-} diffused outward through the liquid film layer and reached the leach solutions.

At the first stage of the leaching process (0 to 4 min), the calcium sulfate product was slightly soluble in water. The calcium sulfate had not yet formed a stable solid film layer on the surface of hydroxyapatite minerals. The leaching process was mainly controlled by the external diffusion liquid film layer. The products of RE^{3+} and PO_4^{3-} diffused easily into the leach solutions, and the overall leaching process speed was relatively fast, resulting in a significant increase on the leaching percentage of REEs.

At the second stage (4 to 30 min), calcium sulfate products gradually formed a stable solid film layer around the hydroxya-

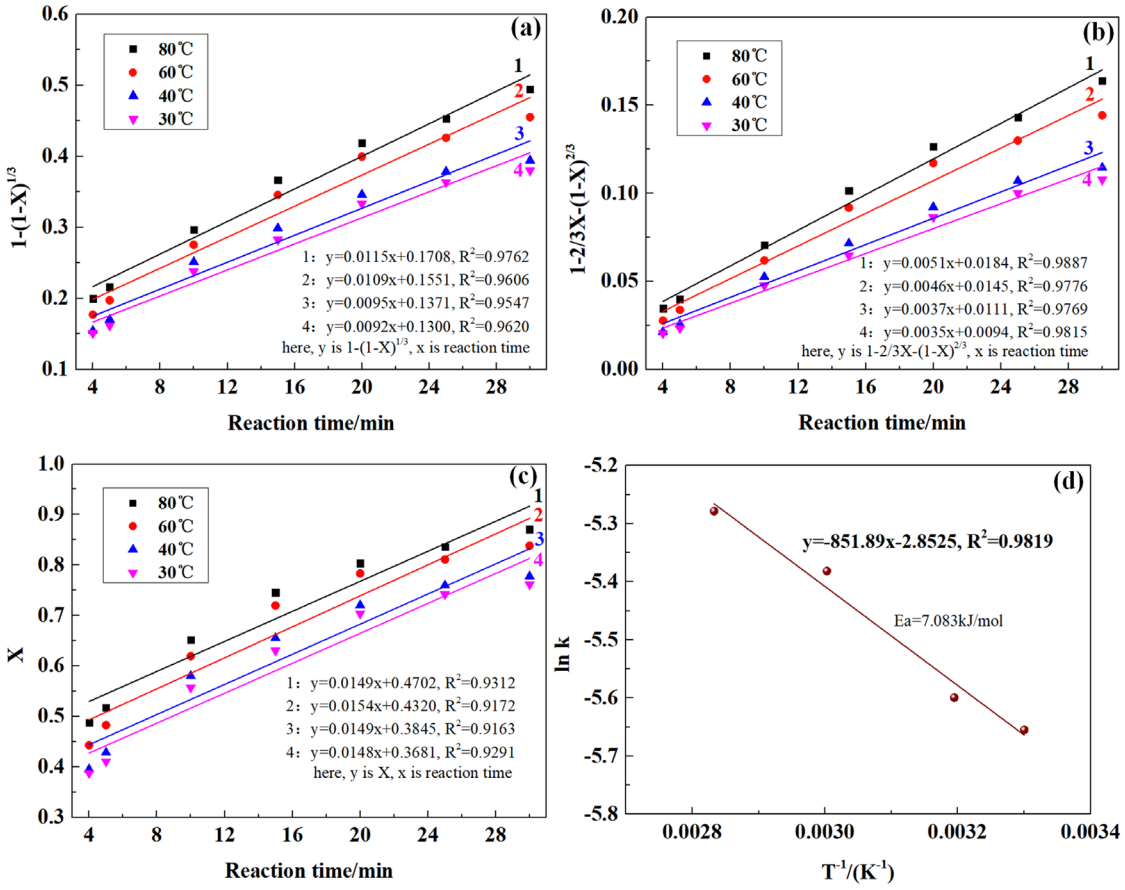

Fig. 4. The results of leaching kinetics for REEs during the sulfuric leaching (4-30 min): (a) Fitting result of $1-(1-X)^{1/3}$ vs t; (b) Fitting result of $1-2/3X-(1-X)^{2/3}$ vs t; (c) Fitting result of X vs t; (d) Calculating activation energy based on Arrhenius Equation

patite minerals, which became increasingly thick. The rate at which the leaching agent and the products of RE^{3+} and PO_4^{3-} passed through this solid film layer gradually slowed, and the leaching process began to be controlled by internal diffusion, resulting in a significant decrease in the leaching rate. As the leaching process continued, the solid film layer of calcium sulfate products became thicker and denser, making it more difficult for the leaching agent and the products of RE^{3+} and PO_4^{3-} to pass through. Finally, when passage through the solid film layer became impossible, the reaction reached equilibrium. This is also consistent with the phenomena reported in our previous research [32]. In the Fig.11 of this literature, we have confirmed that calcium sulfate products gradually coated apatite minerals and finally form phosphogypsum.

Thus, to ensure sufficient acid dosage, appropriately reducing the acid concentration, increasing the reaction temperature, and raising the stirring speed can delay the formation of the calcium sulfate solid layer, thereby enhancing the leaching percentage. These conclusions are consistent with the results of batch tests.

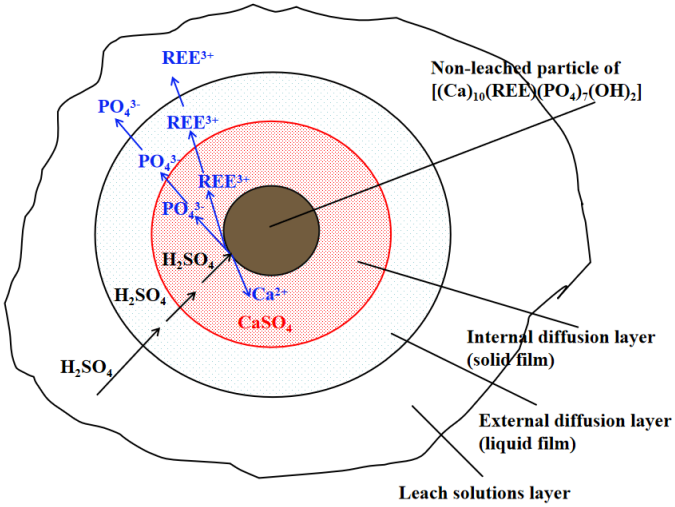

Fig. 5. Shrinking-core model of hydroxyapatite minerals $[(Ca)_{10}(REE)(PO_4)_7(OH)_2]$ in the deep-sea mud during the H_2SO_4 leaching process. Reaction: $(Ca)_{10}(REE)(PO_4)_7(OH)_2 + 2H^+ + 10SO_4^{2-} \rightarrow 10CaSO_4 \downarrow + + 7PO_4^{3-} + 2H_2O + REE^{3+}$

4. Conclusion

This paper conducted a systematic investigation on the sulfuric leaching process of the novel REEs resource of deep-sea mud. The results showed that the REE in deep-sea mud could be leached out via a sulfuric acid leaching process. A optimized REEs leaching percentage of 82.83% was obtained by using 1.0 mol/L sulfuric acid as leaching agents with a liquid-solid ratio of 4:1 at 60°C for 30 min. Under the optimized leaching conditions, the leaching process was conformed to the shrinking-core model which contained two stages as follows: 1) From 0 min to 4 min, the reaction was controlled through an external diffusion process, and could be described as $X = 0.5491 \cdot e^{-4569/RT} \cdot t$ (Ea = 4.569 kJ/mol); 2) From 4 min to 30 min, due to the increase of solid calcium sulfate products, the reaction gradually transformed into an internal diffusion-controlled process, and could be described as $1 - 2/3X - (1 - X)^{2/3} = 0.0577 \cdot e^{-7083/RT} \cdot t$ (Ea = 7.083 kJ/mol).

Acknowledgments

This study was funded by the Ganpo Juncai Support Program.Youth Science and Technology Talent Support Project (2025QT15), GanPo Yingcai Support Program. Youth Innovative leading Talent Support Project (gpyc20240040), National Natural Science Foundation of China (No. 52374354), Ganzhou Key Laboratory project (2024YSPT0001), and Startup Foundation for Doctor Talents of Gannan University of Science and Technology.

REFERENCES

[1] N. Dushyantha, N. Batapola, I.M.S.K. Ilankoon, S. Rohitha, R. Premasiri, B. Abeysinghe, N. Ratnayake, K. Dissanayake, The story of rare earth elements (REEs): Occurrences, global distribution, genesis, geology, mineralogy and global production. Ore Geol. Rev. **122**, 103521 (2020).
DOI: https://doi.org/10.1016/j.oregeorev.2020.103521

[2] A.S. Patil, A.V. Patil, C.G. Dighavkar, V.A. Adole, U.J. Tupe, Synthesis techniques and applications of rare earth metal oxides semiconductors: A review. Chem. Phys. Lett. **796**, 139555 (2022).
DOI: https://doi.org/10.1016/j.cplett.2022.139555

[3] W. Zhang, A. Noble, Mineralogy characterization and recovery of rare earth elements from the roof and floor materials of the Guxu coalfield. Fuel **270**, 117533 (2020).
DOI: https://doi.org/10.1016/j.fuel.20

[4] M. Keersemaker, Critical raw materials resilience: charting a path towards greater security and sustainability. COM. **474**, 69-82 (2020).
DOI: https://doi.org/10.1007/978-3-030-40268-6_9

[5] J. Ohta, K. Yasukawa, K. Nakamura, K. Fujinaga, K. Iijima, Y. Kato, Geological features and resource potential of deep-sea sediments highly enriched in rare-earth elements in the Central Pacific Basin and the Penrhyn Basin. Ore Geol. Rev. **139** Part A, 104440 (2021).
DOI: https://doi.org/10.1016/j.oregeorev.2021.104440

[6] P. Madureira, H. Brekke, G. Cherkashov, M. Rovere, Exploration of polymetallic nodules in the Area: Reporting practices, data management and transparency. Mar. Policy **70**, 101-107 (2016).
DOI: https://doi.org/10.1016/j.marpol.2016.04.051

[7] A. Pandey, Exploration of deep seabed polymetallic sulphides: Scientific rationale and regulations of the International Seabed Authority. Int. J. Min. Sci. Technol. **23** (3), 457-462 (2013).
DOI: https://doi.org/10.1016/j.ijmst.2013.05.006

[8] R. Watzel, C. Rühlemann, A. Vink, Mining mineral resources from the seabed: Opportunities and challenges. Mar. Policy **114**, 103828 (2020).
DOI: https://doi.org/10.1016/j.marpol.2020.103828

[9] Z. Zhang, Y. Du, L. Gao, Y. Zhang, G. Shi, C. Liu, P. Zhang, X. Duan, Enrichment of REEs in polymetallic nodules and crusts and its potential for exploitation. J. Rare Earths. **30** (6), 621-626 (2012).
DOI: https://doi.org/10.1016/S1002-0721(12)60101-X

[10] N. Toro, P. Robles, R.I. Jeldres, Seabed mineral resources, an alternative for the future of renewable energy: A critical review. Ore Geol. Rev. **126**, 103699 (2020).
DOI: https://doi.org/10.1016/j.oregeorev.2020.103699

[11] A. Hussain, P.D.W. Haughton, P.M. Shannon, E.A. Morris, C.S. Pierce, J. E. Omma, Mud-forced turbulence dampening facilitates rapid burial and enhanced preservation of terrestrial organic matter in deep-sea environments. Mar. Pet. Geol. **130**, 105101 (2021).
DOI: https://doi.org/10.1016/j.marpetgeo.2021.105101

[12] S. Petersen, A. Krätschell, N. Augustin, J. Jamieson, J.R. Hein, M.D. Hannington, News from the seabed-Geological characteristics and resource potential of deep-sea mineral resources. Mar. Policy **70**, 175-187 (2016).
DOI: https://doi.org/10.1016/j.marpol.2016.03.012

[13] K. Yasukawa, J. Ohta, M. Hamada, Q. Chang, H. Nakamura, K. Ashida, Y. Takaya, K. Nakamura, H. Iwamori, Y. Kato, Essential processes involving REE-enrichment in biogenic apatite in deep-sea sediment decoded via multivariate statistical analyses. Chem. Geol. **614**, 121184 (2022).
DOI: https://doi.org/10.1016/j.chemgeo.2022.121184

[14] Y. Kato, K. Fujinaga, K. Nakamura, Y. Takaya, K. Kitamura, J. Ohta, R. Toda, T. Nakashima, H. Iwamori, Deep-sea sediments in the Pacific Ocean as a potential resource for rare-earth elements. Nat. Geosci. **4** (8), 535-539 (2011).
DOI: https://doi.org/10.1038/ngeo1185

[15] K. Iijima, K. Yasukawa, K. Fujinaga, K. Nakamura, S. Machida, Y. Takaya, J. Ohta, S. Haraguchi, Y. Nishio, Y. Usui, T. Nozaki, T. Yamazaki, Y. Ichiyama, A. Ijiri, F. Inagaki, H. Machiyama, K. Suzuki, Y. Kato, Discovery of extremely REY-rich mud in the western North Pacific Ocean. Geochem. J. **50** (6), 557-573 (2016).
DOI: https://doi.org/10.2343/geochemj.2.0431

[16] K. Fujinaga, K. Yasukawa, K. Nakamura, K. Nakamura, S. Machida, Y. Takaya, J. Ohta, S. Araki, H. Liu, R. Usami, R. Maki, S. Haraguchi, Y. Nishio, Y. Usui, T. Nozaki, T. Yamazaki, Y. Ichiyama, A. Ijiri, F. Inagaki, H. Machiyama, K. Iijima, K. Suzuki, Y. Kato, Geochemistry of REY-rich mud in the Japanese Exclusive Economic Zone around Minamitorishima Island. Geochem. J. **50** (6), 575-590 (2016).
DOI: https://doi.org/10.2343/geochemj.2.0432

[17] K. Nakamura, S. Machida, K. Okino, Y. Masaki, K. Iijima, K. Suzuki, Y. Kato, Acoustic characterization of pelagic sediments using sub-bottom profiler data: Implications for the distribution of REY-rich mud in the Minamitorishima EEZ, western Pacific. Geochem. J. **50** (6), 605-619 (2016).
DOI: https://doi.org/10.2343/geochemj.2.0433

[18] Y. Takaya, K. Yasukawa, T. Kawasaki, K. Fujinaga, J. Ohta, Y. Usui, K. Nakamura, J.I. Kimura, Q. Chang, M. Hamada, G. Dodbiba, T. Nozaki, K. Iijima, T. Morisawa, T. Kuwahara, Y. Ishida, T. Ichimura, M. Kitazume, T. Fujita, Y. Kato, The tremendous potential of deep-sea mud as a source of rare-earth element. Sci. Rep. **8**, 5763 (2018).
DOI: https://doi.org/10.1038/s41598-018-23948-5

[19] J. Li, X. Shi, M. Huang, M. Yu, D. Bi, Z. Song, F. Shen, J. Liu, Y. Zhang, H. Wang, Y. Sun, F. Shi, The transformation and accumulation mechanism of rare earth elements in deep-sea sediments from the Wharton Basin, Indian Ocean. Ore Geol. Rev. **161**, 105655 (2023).
DOI: https://doi.org/10.1016/j.oregeorev.2023.105655

[20] Y. Liu, Y. Jing, W. Zhao, Distribution of rare earth elements and implication for Ce anomalies in the clay-sized minerals of deep-sea sediment, Western Pacific Ocean. Appl. Clay Sci. **235**, 106876 (2023). DOI: https://doi.org/10.1016/j.clay.2023.106876

[21] A. Menendez, R.H. James, S. Roberts, K. Peel, D. Connelly, Controls on the distribution of rare earth elements in deep-sea sediments in the North Atlantic Ocean. Ore Geol. Rev. **87**, 100-113 (2017).
DOI: https://doi.org/10.1016/j.oregeorev.2016.09.036

[22] E. Tanaka, K. Nakamura, K. Yasukawa, K. Mimura, K. Fujinaga, J. Ohta, K. Iijima, T. Nozaki, S. Machida, Y. Kato, Chemostratigraphic correlations of deep-sea sediments in the western North Pacific Ocean: A new constraint on the distribution of mud highly enriched in rare-earth elements. Minerals **10** (6), 575 (2020).
DOI: https://doi.org/10.3390/min10060575

[23] X. Zhang, C. Tao, X. Shi, H. Li, M. Huang, D. Huang, Geochemical characteristics of REY-rich pelagic sediments from the GC02 in central Indian Ocean Basin. J. Rare Earth. **35**, 1047-1058 (2017).
DOI: https://doi.org/10.1016/S1002-0721(17)61012-3

[24] D. Bi, X. Shi, M. Huang, M. Yu, T. Zhou, Y. Zhang, A. Zhu, M. Shi, X. Fang, Geochemical and mineralogical characteristics of deep-sea sediments from the western North Pacific Ocean: Constraints on the enrichment processes of rare earth elements. Ore Geol. Rev. **138**, 104318 (2021).
DOI: https://doi.org/10.1016/j.oregeorev.2021.104318

[25] X. Shi, Y. Fu, B. Li, M. Huang, X. Ren, J. Liu, M. Yu, C. Li, Research on deep-sea minerals in China: Progress and discovery (2011-2020). Bull. Mineral. Petrol. Geochem. **40** (2), 305-318 (2021).
DOI: https://doi.org/10.19658/j.issn.1007-2802.2021.40.022

[26] E. Tanaka, K. Nakamura, K. Yasukawa, K. Mimura, K. Fujinaga, K. Iijima, T. Nozaki, Y. Kato, Chemostratigraphy of deep-sea sediments in the western North Pacific Ocean: Implications for genesis of mud highly enriched in rare-earth elements and yttrium. Ore Geol. Rev. **119**, 103392 (2020).
DOI: https://doi.org/10.1016/j.oregeorev.2020.103392

[27] T. Wang, Y. Dong, F. Chu, W. Zhang, X. Li, R. Su, L. Tian, In situ strontium isotope stratigraphy of fish teeth in deep-sea sediments from the western Clarion-Clipperton Fracture Zone, eastern Pacific Ocean. Chem. Geol. **636**, 121624 (2023).
DOI: https://doi.org/10.1016/j.chemgeo.2023.121624

[28] K. Zhang, Z. Liu, H. Liu, W. Zhu, B. Wei, X. Zhong, R. Wang, Y. Zeng, Hydrochloric acid leaching of rare earth elements from a novel source of deep-sea sediments and advantage of reduction with H_2O_2. Hydrometallurgy. **230**, 106383 (2024).
DOI: https://doi.org/10.1016/j.hydromet.2024.106383.

[29] X. Feng, Z. Long, D. Cui, L. Wang, X. Huang, G. Zhang, Kinetics of rare earth leaching from roasted ore of bastnaesite with sulfuric acid. Transactions of Nonferrous Metals Society of China. **23** (3), 849-854 (2013).
DOI: http://doi.org/10.1016/S1003-6326(13)62538-8

[30] H. Li, Principles of Metallurgy (Second Edition), Science Press, Beijing, PP 279-281 (2018).

[31] A.Z. Sari, M. Turan, Investigation of atmospheric pressure leaching conditions and leaching kinetics in the obtaining of industrial copper (II) acetate solution from copper slags. Journal of Central South University **30** (8), 2556-2573 (2023).
DOI: https://doi.org/10.1007/s11771-023-5406-5

[32] K. Zhang, B. Wei, J. Tao, X. Zhong, W. Zhu, R. Wang, Z. Liu, Recovery of rare earth elements from deep-sea mud using acid leaching followed by selective solvent extraction with N1923 and TBP. Separation and Purification Technology **318**, 124013 (2023).
DOI: https://doi.org/10.1016/j.seppur.2023. 124013